Effects of Co and Ni on visible light photocatalytic properties of layered double hydroxide films

Huan Yu, Wei-Wei Wang ✉, *Jiao Li, Ri-Min Cong*

School of Material Science and Engineering, Shandong University of Technology, Zibo City, Shandong 255049, People's Republic of China
✉ *E-mail: wangweiwei@sdut.edu.cn*

Published in Micro & Nano Letters; Received on 3rd December 2017; Accepted on 7th December 2017

Altering the composition of layered double hydroxides (LDHs) is an effective method for changing their properties. In this study, LDH films with different compositions were fabricated on conductive cloth by using a hydrothermal method. Electron microscopy, X-ray diffraction, and UV–vis diffuse reflectance spectroscopy were used to investigate the morphology, crystal structure, and optical properties of the LDH films. The photocatalytic activity of LDHs with different compositions in the degradation of methyl orange was investigated under visible light irradiation. Our experimental results show that the reductive sites (Ni(II) and Co(II)) of LDHs and the conductive substrate improve the separation of photogenerated charges and prevent the particle aggregation of LDHs. LDH films (NiAl-LDHs, NiFe-LDHs, and CoAl-LDHs) with reductive sites (Ni(II) and Co(II)) exhibit higher visible light photocatalytic performance.

1. Introduction: Semiconductor photocatalysis offers the potential for complete elimination of toxic chemicals through its efficiency and potentially broad applicability. However, the fast recombination rate of the photogenerated electron/hole pairs and the low use of visible light limit its large-scale practical application [1]. To overcome this limitation, various methods have been carried out for improving the quantum efficiency, such as doping and composite [2, 3]. However, for the charges to be efficiently separated, these efforts generally require complicated reaction steps and longer reaction time.

Compared to composites with different units, the properties of layered double hydroxides (LDHs) can be changed by simply varying their chemical compositions. The general formula of LDHs is $[M^{2+}_{1-x}M^{3+}_{x}(OH)_2](A^{n-})_{x/n}{\cdot}yH_2O$, where M^{2+} and M^{3+} represent divalent and trivalent cations, respectively. The chemical composition of LDHs can be varied by using different divalent metal ions (such as Mg^{2+}, Ni^{2+}, and Co^{2+}) and trivalent metal ions (such as Al^{3+}, Fe^{3+}, and Cr^{3+}). Studies have reported that reductive sites can offer an effective pathway for electron–hole transport [4, 5]. For example, the reductive Co(II) sites in CoAl-LDHs helped to capture leached Pd(II) species through an in situ redox reaction, resulting in monodispersed Pd nanoclusters on the surface of the CoAl-LDHs. The obtained CoAl-LDH/Pd composites had excellent stability and recyclability [6]. The Cr^{3+} in Au/Cr-substituted hydrotalcite (Au/Cr-HT) could form the Cr^{3+}–Cr^{6+} redox cycle and make Au/Cr-HT an efficient heterogeneous catalyst for aerobic alcohol oxidation [7]. From this viewpoint, the reductive sites (Co(II), Ni(II)) in LDHs may provide a new means of capturing and separating photogenerated electron–hole pairs and thus improving the photocatalytic activity of LDHs. In addition, owing to their charged layer structure, LDHs tend to aggregate during preparation, which decreases their photocatalytic activity. Using a two-dimensional structure with excellent carrier mobility as the substrate is an effective approach for enhancing the photocatalytic efficiency by preventing particle agglomeration and decreasing charge recombination [8]. The present Letter illustrates a simple hydrothermal method for preparing LDH films with different compositions on the surface of conductive cloth. The activity of the films in the degradation of methyl orange under visible light irradiation and the effects of the reductive sites of LDHs on the photocatalytic properties were investigated. The formation of LDH films on the surface of the substrate was observed to facilitate sample recycling.

2. Experimental: To prepare NiAl-LDH films, $Ni(NO_3)_2{\cdot}6H_2O$ (0.15 mol/L), $Al(NO_3)_3{\cdot}9H_2O$ (0.05 mol/L), NH_4F (0.2 mol/L), and urea (0.5 mol/L) were dissolved in deionised water and stirred to form a clear solution. The conductive cloth (2 cm × 6 cm) was cleaned with a mixture solution (the volume ratio of deionised water, ethanol and acetone was 1:1:1) in an ultrasound bath for 30 min and then deionised water to ensure the surface was cleaned. Then the conductive cloth was oriented vertically in the solution at 110°C for 8 h without stirring. After the reaction, a thin film formed on the bottom side of the conductive cloth. For NiFe-LDH films, $Fe(NO_3)_3{\cdot}9H_2O$ (0.05 mol/L) was used instead of $Al(NO_3)_3{\cdot}9H_2O$. For CoAl-LDH films, $Co(NO_3)_2{\cdot}6H_2O$ (0.15 mol/L) was used instead of $Ni(NO_3)_2{\cdot}6H_2O$. For MgAl-LDH films, $Mg(NO_3)_2{\cdot}6H_2O$ (0.15 mol/L) was used instead of $Ni(NO_3)_2{\cdot}6H_2O$, and the reaction temperature was increased to 140°C. For LDH films on the surface of non-woven fabrics, non-woven fabrics were used as the substrate instead of the conductive cloth.

X-ray powder diffraction (XRD) patterns were recorded using a D8 ADVANCE X-ray diffractometer with Cu K_α radiation ($\lambda = 1.5406$ Å). The scanning electron microscopy (SEM) images were recorded on an FEI-Sirion200 field emission scanning electron microscope. The transmission electron microscopy (TEM) images, high-resolution transmission electron microscopy (HRTEM) images and the energy dispersive spectroscopy (EDS) spectra were taken with a JEOL JEM-2100F field emission transmission electron microscope. The TEM samples were obtained by peeled off LDHs from the substrate. Photocatalytic reactions were carried out using a 300 W Xe lamp with 420 nm cutoff filter as the light source. The UV–vis diffuse reflectance spectroscopy was recorded by a UV–vis spectrophotometer (UV-3600, Shimadzu). Fourier transform infrared (FTIR) spectroscopy was obtained on a Thermo Nicolet 5700. Photoluminescence (PL) spectra at 385 nm were investigated using Hitachi F-2500 FL spectrophotometer comprising of a Xe lamp as excitation source.

Photocatalytic property measurement: LDH film (2 cm × 6 cm) was immersed in 40 mL of methyl orange solution (50 mg/L) and kept in the dark for 30 min to ensure adsorption–desorption equilibrium. Analytical samples were removed from the reaction solution after various visible light irradiation times and analysed using a UV–vis spectrophotometer at 464 nm.

Adsorption property measurement: LDH film (2 cm × 6 cm) was immersed in 40 mL of methyl orange solution with different initial

doi: 10.1049/mnl.2017.0836

concentrations (10, 30, 50, 70, 90 and 110 mg/L) at room temperature for 48 h. The amount of methyl orange adsorbed at equilibrium (q_e, mg/g) was calculated from formula: $q_e = (C_0 - C_e)V/m$, where C_0 and C_e represent the concentration of methyl orange (mg/L) before and after removal process, respectively. V is the solution volume (0.04 L) and m is the weight of the adsorbent (g). The weight of the adsorbent was calculated from formula $m = m_t - m_0$, where m_0 and m_t represent the weight of substrate before and after LDH growth, respectively.

3. Results and discussion: The crystal structure and phase composition of the as-prepared LDHs were confirmed from XRD patterns (Fig. 1). The structures of all the samples match the typical LDH lamellar structure well (JCPDS File No. 51-1525, 51-0463, Figs. 1*a–d*). According to the (003) and (006) reflections, the basal spacing values are 0.7797 nm (NiAl-LDHs), 0.7810 nm (NiFe-LDHs), 0.7722 nm (CoAl-LDHs), and 0.7702 nm (MgAl-LDHs), which coincide well with the values for NO_3^- intercalated LDH materials. In addition, MgAl-LDHs prepared at a high reaction temperature (140°C) exhibit the highest crystallinity. For MgAl-LDHs, if the reaction temperature was low (at 110°C), the main phase was aluminium fluoride hydroxide (JCPDS File No. 41-0381, Fig. 1*e*). No layer structured LDHs was observed.

Fig. 2*a* shows the NiAl-LDH sheets intersecting and aligned vertically on the conductive cloth. They coat the surface of the cloth uniformly, have a porous structure, and are ~50 nm thick. The lateral dimensions of the NiAl-LDH sheets are up to 100 nm (Fig. 2*e*). The NiFe-LDH and MgAl-LDH films exhibit similar sheet-like morphology, but the NiFe-LDH films are thicker (~70 nm, Figs. 2*b* and *c*). When the M(II) of the LDHs is changed from Ni^{2+} to Co^{2+}, the CoAl-LDHs exhibit a different morphology, with a tightly connected structure and uniform coating of the substrate (inset in Fig. 2*d*). The sheets are transparent to the electron beam, suggesting that they are very thin (Fig. 2*h*). The CoAl-LDH sheets tend to roll up, forming a rod-like shape (inset in Fig. 2*h*), consistent with the preceding SEM analysis. All the HRTEM images taken from one sheet can be indexed to the (012) plane, which matches the reported values of the hexagonal LDH structure well (insets in Figs. 2*e–h*). EDS spectra (Fig. 1*S*) also confirmed the compositions of LDH film were Ni and Al (for NiAl-LDH), Ni and Fe (for NiFe-LDH), Mg and Al (for MgAl-LDH), and Co and Al (for Co-LDH), respectively.

Fig. 3*a* shows the room temperature UV–vis diffuse reflectance spectra. The band gap energies calculated on the basis of the corresponding absorption edges are 2.25 eV (NiAl-LDHs), 2.16 eV (NiFe-LDHs), 2.01 eV (CoAl-LDHs), and 2.86 eV (MgAl-LDHs). All of the LDH films were confirmed to be visible-light-driven photocatalysts.

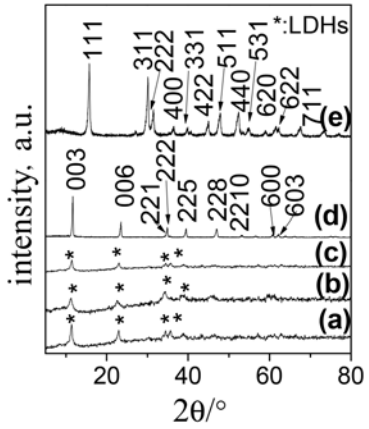

Fig. 1 *XRD patterns*
a NiAl-LDHs
b NiFe-LDHs
c CoAl-LDHs
d MgAl-LDHs
e MgAl-LDHs prepared at 110°C for 8 h

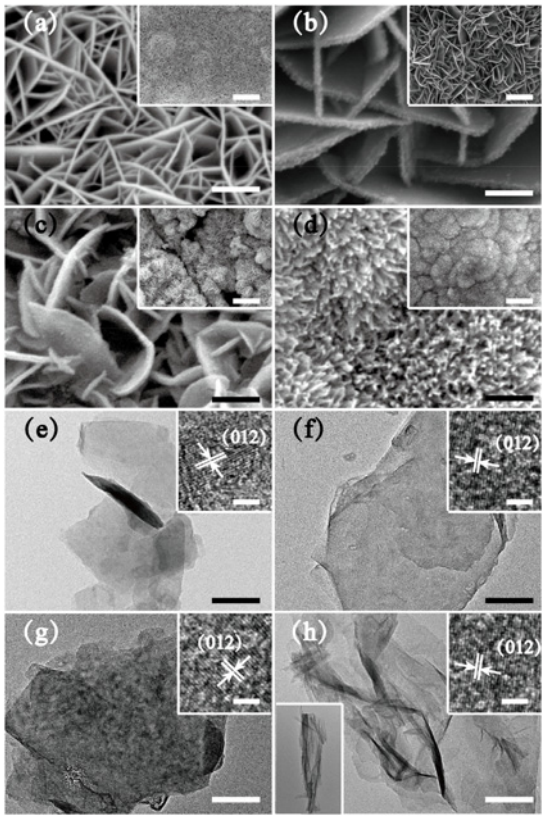

Fig. 2 *SEM images*
a NiAl-LDHs
b MgAl-LDHs
c NiFe-LDHs
d CoAl-LDHs, scale bar:500 nm; insets: low-magnification SEM images, scale bar: 5 μm. TEM images of
e NiAl-LDHs
f MgAl-LDHs
g NiFe-LDHs
h CoAl-LDHs, scale bar: 100 nm; insets: high-magnification TEM images, scale bar: 2 nm. The lower left inset of Fig. 2*h*: high-magnification TEM image

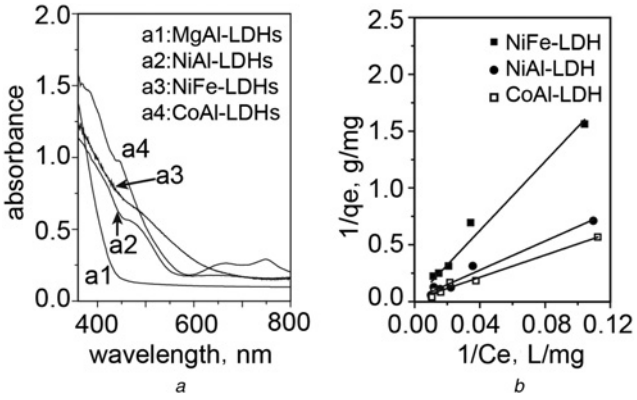

Fig. 3 *DRS spectra and adsorption ability*
a Room temperature UV–vis diffuse reflectance spectra
b Adsorption isotherms of methyl orange, solid lines refer to the linear fit

In general, adsorption is the necessary prerequisite to the photocatalytic reaction. A blank experiment without the irradiation demonstrated that only a small quantity of methyl orange was adsorbed. The adsorption ratio was <6% for NiAl-LDHs, NiFe-LDHs and CoAl-LDHs (Fig. 4*a*). CoAl-LDHs show a higher adsorption rate within the first 40 min. The adsorption rate remains constant with increasing time. To evaluate methyl orange adsorption process of LDH film, the adsorption isotherm was conducted (Fig. 3*b*). The experimental data fitted well to the Langmuir adsorption model ($1/q_e = 1/(q_m b C_e) + 1/q_m$). The regression coefficient (R^2) was 0.969 (NiAl-LDHs), 0.966 (NiFe-LDHs) and 0.976 (CoAl-LDHs), respectively. The maximal methyl orange removal capacity (q_m) was 44.31 mg/g for NiAl-LDHs, 51.52 mg/g for NiFe-LDHs, 52.35 mg/g for CoAl-LDHs within our experimental range. NiAl-LDHs, NiFe-LDHs and CoAl-LDHs show the similar methyl orange adsorption behaviour, which is a single layer adsorption process.

The photocatalytic activity in methyl orange photodegradation under visible light irradiation was evaluated (Fig. 4*a*, C_0 and C_t are the equilibrium concentrations of methyl orange before and after irradiation). CoAl-LDH films show a rapid degradation ratio within 40 min of irradiation. With increasing irradiation time, the degradation ratio for CoAl-LDH, NiAl-LDH and NiFe-LDH tends to the same. Combined with the above adsorption analysis, the different adsorption ratio led to the different activity within first 40 min irradiation. The degradation of methyl orange could reach 91% in the presence of the NiAl-LDH films after 120 min of irradiation. The NiFe-LDH and CoAl-LDH films exhibit photocatalytic activity similar to that of the NiAl-LDH films. However, the photocatalytic activity of the MgAl-LDH films is lower, and the degradation ratio is 24.1%. The maximum degradation rate $(dC/dt)_{max}$ (the maximum slope point of the fitted curves) and the half degradation time $t_{1/2}$ are used to evaluate the catalyst activity [9]. The $(dC/dt)_{max}$ is 2.412, 2.029, 2.198 and 0.538 for NiAl-LDHs, NiFe-LDHs, CoAl-LDHs and MgAl-LDHs, respectively. $t_{1/2}$ are 20, 23, 22 and 31 min for NiAl-LDHs, NiFe-LDHs, CoAl-LDHs and MgAl-LDHs, respectively. The higher $(dC/dt)_{max}$ and the lower $t_{1/2}$ confirmed that NiAl-LDHs, NiFe-LDHs and CoAl-LDHs exhibited the better photocatalytic efficiency than that of MgAl-LDHs. The LDH films with Ni^{2+} (or Co^{2+}) in the M^{2+} position exhibit higher photocatalytic activity.

We also used FTIR spectra to investigate LDHs film before and after photocatalytic (and adsorption) experiments (Fig. 4*b*). Peaks at 3500 cm^{-1} around and 1650 cm^{-1} are the absorption from hydroxyl stretching vibration, which represents the existing of –OH and H_2O. Peaks at 1370 cm^{-1} confirmed that the interlayer ions for LDHs films were NO_3^-. After photocatalytic degradation of methyl orange, the peak intensity of NO_3^- decreased and no obvious peaks for methyl orange were observed. While LDHs after adsorption experiments show some peaks for methyl orange. The difference of FTIR spectra between photocatalytic experiments and adsorption experiments confirmed that the degradation of methyl orange in the presence of LDH films under irradiation was not through adsorption.

In general, the photocatalytic activity of materials is related to the particle size, exposed planes, and band gaps. According to the preceding analysis, MgAl-LDHs have poorer photocatalytic properties compared with NiAl-LDHs and CoAl-LDHs even though they have the same sheet-like shape and exposed planes ((012)). The main difference among them is their composition. The high recombination rate of photogenerated electron–hole pairs hinders photocatalytic activity. Introducing electron traps or hole traps by doping and preparing composites are common methods for separating photogenerated electron–hole pairs.

In our experiments, electron–hole pair recombination was suppressed by adjusting the composition of LDHs. Owing to the reductive nature of metal ions such as Ni(II) and Co(II) in LDHs, the reductive M(II) sites could act as photogenerated charge traps and increase the charge separation [3, 7]. For comparison, LDH films on the surface of non-woven fabrics were prepared. All of these LDHs film grown on the surface of non-woven fabrics show the similar morphology to that of LDH films on the surface of conductive cloth (Fig. 5). The structures of these films match the typical LDH lamellar structure well (Fig. 6*a*). However, they showed lower photocatalytic activity (Fig. 6*b*), which confirmed that the substrate with high electroconductivity facilitates the efficient transportation of photogenerated charges among the LDHs [10]. Studies have reported that the recombination of photogenerated charges can

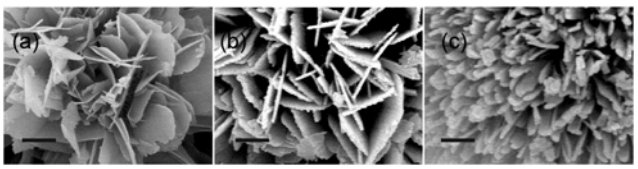

Fig. 5 *SEM images of LDH films grown on the surface of non-woven fabrics*
a NiAl-LDH film
b NiFe-LDH film
c CoAl-LDH film, scale bar: 1 μm

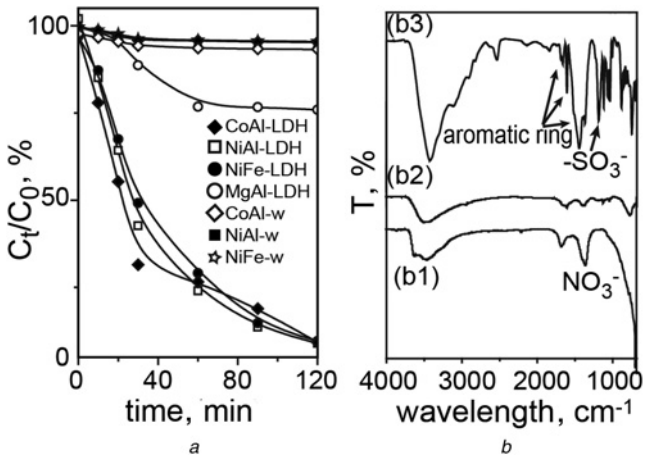

Fig. 4 *Photocatalytic activity*
a Photocatalytic activity under visible-light irradiation for LDH films grown on the surface of conductive cloth, NiAl-w, NiFe-w and CoAl-w represent the blank experiments adding photocatalysts without irradiation
b FTIR spectra of NiAl-LDH film (b1) before and (b2) after photocatalytic experiments, (b3) After adsorption experiments

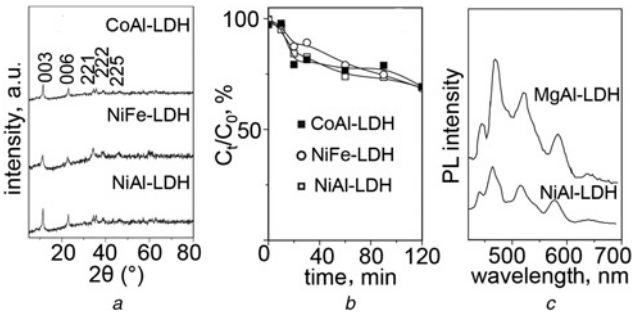

Fig. 6 *Photocatalytic mechanism*
a XRD patterns
b Photocatalytic activity under visible-light irradiation of LDH films grown on the surface of non-woven fabrics
c Emission spectra at 385 nm for LDH films grown on the surface of conductive cloth

doi: 10.1049/mnl.2017.0836

be investigated through PL spectroscopy [10, 11]. For band–band PL emission, the lower the PL intensity is, the higher the separation rate of the photogenerated charges. The emission intensity of NiAl-LDHs was lower than that of MgAl-LDHs, and hence, a higher photocatalytic activity was observed, confirming that the reductive sites (Co(II) and Ni(II)) of LDHs enhance their photocatalytic activity (Fig. 6*c*).

4. Conclusion: LDH films with different compositions were prepared using a hydrothermal method. All LDH films have a sheet-like morphology and are aligned vertically on the conductive cloth. For the degradation of methyl orange, LDH films with reductive sites (Co or Ni) exhibit higher photocatalytic activity, owing to the photogenerated carriers having a longer lifetime for participating in photocatalytic reactions.

5. Acknowledgment: This work was supported by Shandong Provincial Natural Science Foundation of China (grant no. ZR2015BM022).

6 References

[1] Sheng X., Liu Z., Zeng R., *ET AL.*: 'Enhanced photocatalytic reaction at air–liquid–solid joint interfaces', *J. Am. Chem. Soc.*, 2017, **139**, (36), pp. 12402–12405

[2] Huang H.M., Dai B.Y., Wang W., *ET AL.*: 'Oriented built-in electric field introduced by surface gradient diffusion doping for enhanced photocatalytic H_2 evolution in CdS nanorods', *Nano Lett.*., 2017, **17**, (6), pp. 3803–3808

[3] Qu J., He X., Li X., *ET AL.*: 'Precursor preparation of Zn–Al layered double hydroxide by ball milling for enhancing adsorption and photocatalytic decoloration of methyl orange', *RSC Adv.*, 2017, **7**, pp. 31466–31474

[4] Han J.B., Dou Y.B., Zhao J.W., *ET AL.*: 'Flexible CoAl LDH@PEDOT core/shell nanoplatelet array for high-performance energy storage', *Small*, 2013, **9**, (1), pp. 98–106

[5] Xu S.M., Pan T., Dou Y.B., *ET AL.*: 'Theoretical and experimental study on $M^{II}M^{III}$-layered double hydroxides as efficient photocatalysts toward oxygen evolution from water', *J. Phys. Chem. C*, 2015, **119**, (33), pp. 18823–18834

[6] Li P., Huang P.P., Wei F.F., *ET AL.*: 'Monodispersed Pd clusters generated in situ by their own reductive support for high activity and stability in cross-coupling reactions', *J. Mater. Chem. A*, 2014, **2**, pp. 12739–12745

[7] Liu P., Degirmenci V., Hensen E.J.M.: 'Unraveling the synergy between gold nanoparticles and chromium-hydrotalcites in aerobic oxidation of alcohols', *J. Catal.*, 2014, **313**, pp. 80–91

[8] Lan M., Fan G.L., Yang L., *ET AL.*: 'Significantly enhanced visible-light-induced photocatalytic performance of hybrid Zn–Cr layered double hydroxide/graphene nanocomposite and the mechanism study', *Ind. Eng. Chem. Res.*, 2014, **53**, (33), pp. 12943–12952

[9] D'Arienzo M., Crippa M., Essawy A.A., *ET AL.*: 'Membrane-assisted charge separation and photocatalytic activity in embedded TiO_2: a kinetic and mechanistic study', *J. Phys. Chem. C*, 2010, **114**, pp. 15755–15762

[10] Chowdhury P.R., Bhattacharyya K.G.: 'Ni/Co/Ti layered double hydroxide for highly efficient photocatalytic degradation of rhodamine B and acid Red G: a comparative study', *Photochem. Photobiol. Sci.*, 2017, **16**, pp. 835–839

[11] Baliarsingh N., Parida K.M., Pradhan G.C.: 'Effects of Co, Ni, Cu, and Zn on photophysical and photocatalytic properties of carbonate intercalated MII/Cr LDHs for enhanced photodegradation of methyl orange', *Ind. Eng. Chem. Res.*, 2014, **53**, (10), pp. 3834–3841